Periodicals of Engineering and Natural Sciences ISSN 2303-4521
Vol. 8, No. 2, June 2020, pp.1011-1023

The determination of ground granulated concrete compressive strength-based machine learning models

Mohammed H. Mohana[1]
[1] College of civil engineering, University of Anbar

ABSTRACT

The advancement of machine learning (ML) models has received remarkable attention by several science and engineering applications. Within the material engineering, ML models are usually utilized for building an expert system for supporting material design and attaining an optimal formulation material sustainability and maintenance. The current study is conducted on the base of the utilization of ML models for modeling compressive strength (C_s) of ground granulated blast furnace slag concrete (GGBFSC). Random Forest (RF) model is developed for this purpose. The predictive model is constructed based on multiple correlated properties for the concrete material including coarse aggregate (CA), curing temperature (T), GGBFSC to total binder ratio (GGBFSC/B), water to binder ratio (w/b), water content (W), fine aggregate (FA), superplasticizer (SP). A total of 268 experimental dataset are gather form the open-source previous published researches, are used to build the predictive model. For the verification purpose, a predominant ML model called support vector machine (SVM) is developed. The efficiency of the proposed predictive and the benchmark models is evaluated using statistical formulations and graphical presentation. Based on the attained prediction accuracy, RF model demonstrated an excellent performance for predicting the C_s using limited input parameters. Overall, the proposed methodology showed an exceptional predictive model that can be utilized for modeling compressive strength of GGBFSC.

Keywords: Compressive strength prediction, granulated blast furnace slag concrete, variability performance, machine learning models, random forest.

Corresponding Author: **Mohammed Hmood Mohana**

Mohana,
Departement of civil engineering,
University of Anbar,
E-mail: mhm1961mhm@uoanbar.edu.iq

1. Introduction

The enhancement of the sustainability of concrete has been the focus of several studies with the aim of reducing the level of CO_2 generation from cement production, as well as increasing the durability of concrete; the researchers believe that these measures can be beneficial to the environment through the reduction of waste and conservation of resources [1]–[3]. The commonest approach towards achieving these aims is the utilization of recycled aggregates & mineral additives such as ground granulated blast furnace slag, fly ash, and silica fume [4]. These materials are used as partial replacement for either aggregates or cement during cement production [1], [5], [6]. Studies have shown that the incorporation of these materials into concretes improves the durability and mechanical properties of the resulting concrete, reduces the emission of CO_2, conserves energy, and reduces the harsh impact of concrete on the environment [7], [8]. During the production of iron in a furnace, blast furnace slag (BFS) is generated as the waste product. The molten BFS is cooled with water and pulverized to form GGBFS which, in the presence of water, can react with (Ca(OH)2) to form calcium silicate hydrate. This product is mainly responsible for the strength of most cement-based compounds [9], [10]. This pozzolanic reaction of GGBFS makes its use as a cement replacement material capable of reducing the early strength; however, it improves the ultimate strength, durability, and microstructure of hardened concrete [11]–[13].

There are several available mathematical models and empirical equations for the estimation of the compressive strength (C_S) and other properties of concrete; these models were developed to reduce the experimental task involved in designing concrete mixtures [14]–[17]. Generally, these equations are regression equations that are reliant on the outcome of several experiments. Meanwhile, the selection of a suitable regression equation for any analysis demands experience and numerous techniques since accuracy is inversely related to the number of explanatory variables in such experiments. The recent times have seen the numerical modeling of such relationships achieved by building an intelligent models which can learn and generalize from instances via trial-and-error without requiring any assumptions [18]–[22]. Among several ML models, artificial neural network (ANN) which is characterized by the ability to generate accurate solutions and evidential results even when there is insufficient data [23]–[25]. Several other ML models have been implemented for concrete compressive strength modeling with an optimistic manner [26]–[30]. Other literature review studies, for instance, the study by Bilim et al (2009) reported the use of ANN model trained with numerous learning algorithms for the prediction of the C_S of GGBFSC based on the components of the concrete and the age [31]. Another study by Boukhatem et al (2011) focused on the use of ANN for the estimation of the efficiency factor of GGBFS related with concrete strength [32]. Numerous other ML have been applied in various studies for the prediction of the C_S and other concrete properties [7], [31], [33], [34].

Although, there have a massive researches on the application of ANN or even SVM models, those models are associated with certain disadvantages, such as easily entrapment in local minima based on the initial parameters' selection; it may also be unreliable as its prediction accuracy is normally low [35], [36]. Scholars devoted several attempts to overcome these problems by exploring new models that are more reliably applicable to solve this complex problem of prediction. For example, the hybridization of ANN model with other metaheuristics have been suggested and among such metaheuristics, particle swarm optimization algorithms has been the commonly considered algorithm for combination with ANN due to its wide applicability and simplicity [37]. The hybridized ML models are relied on the global search capability of metaheuristics algorithms and to ensure the convergence to the global optima in a faster manner compared to the standalone ML models. The research scope of this area is still the stage of the exploration of more robust and simple ML models. Hence, the current study is explored the capacity of the RF model for modeling the C_S of ground granulated blast furnace slag concrete. The performance of the RF model is validated against SVM model. Different input combination based on the related parameters are constructed in accordance to the degree of correlation.

2. Data description

The development of the proposed RF and the SVM models for the prediction of the C_S of GCBFSC, it is important to ensure the data is prepared and that the database for the training and testing of the prediction model is constructed. In this study, the 268 experimental dataset were used, in which were collected from several published studies [15], [38]–[42]. All these data contained all the related information to the main characteristics of concrete and experimental C_S of GGBFSC. The selection of the variables was based on correlation statics that generated seven input combinations. The considered input parameters were the curing temperature (T), GGBFS-to-total-binder ratio (GGBFSC/B), water-to-binder ratio (w/b), water (W), coarse aggregate (CA), fine aggregate (FA), and superplasticizer (SP), while the output variable was the compressive strength at 28 days of age that is in the range of 17 - 80 MPa.

3. Methodological overview

3.1. Random forest model

Random forest model (RF) is commonly used in classification and regression problems; it works by constructing several random trees and relies on the bootstrapping method [43], [44]. The role of the RF in regression tasks involves the division of the input variables into several parts and computing the error between the actual and the predicted values. The sum of squared errors (SSE) for each part is computed and the best part is selected based on the minimum SSE. The samples are chosen randomly during the training process and the ones that were not selected are called out-of-bag samples which are used for the selection of the most significant variable based on the accuracy of the predicted output [45].

In the RF, the hyper-parameters consists of the number of trees in the forest, as well as the minimum required samples at a leaf node [46]. These hyper-parameters are tuned on the 75% dataset using 10-fold cross validation; this involves random splitting of the 75% dataset in each fold into 10 subsets. Out of these 10 subsets, 9 subsets are used to search for the optimum RF hyper-parameters for 40 times; the root mean square error (RMSE) value is computed each time on the other subset. The RF model with the least RMSE is selected at the end of 40 iterations based on the validation set. However, the best RF model with the optimum hyper-parameters is selected after 10 folds. Being that the procedure itself can cause the validation set to overfit, it is necessary to confirm the performance of the selected RF model in terms of its performance on the 25% dataset.

3.2. Support vector machine (SVM)

Support vector machine (SVM) is a supervised method for establishing the input-output relationship when building predictive models. The SVM is mainly peculiar in its kernel function, absence of local minima through learning process, and control system via organized support vectors and margin value [47]. The input variables in SVM are transformed into high dimensional space using nonlinear kernel function as depicted in Figure 1 [48].

With this transformation, the algorithm can select the best hyperplane ($(Y_i = \omega_0 + \sum_{i=1}^{m} \omega_i \, \phi(x))$) that will separate the data set. This feature confers SVM with the capability to handle both linear and nonlinear functions. The SVM model has shown capability in achieving the optimal point in learning process when compared with another algorithm such as ANN. However, there are certain drawbacks of the SVM model when faced with large data set; such problems are related with the requirement of memory and kernel function selection. Initially, SVM was proposed by [49] for handling classification tasks. However, the introduction of ε – insensitive loss function by [50] expanded the application of the SVM to regression tasks as shown in Figure 2 [51].

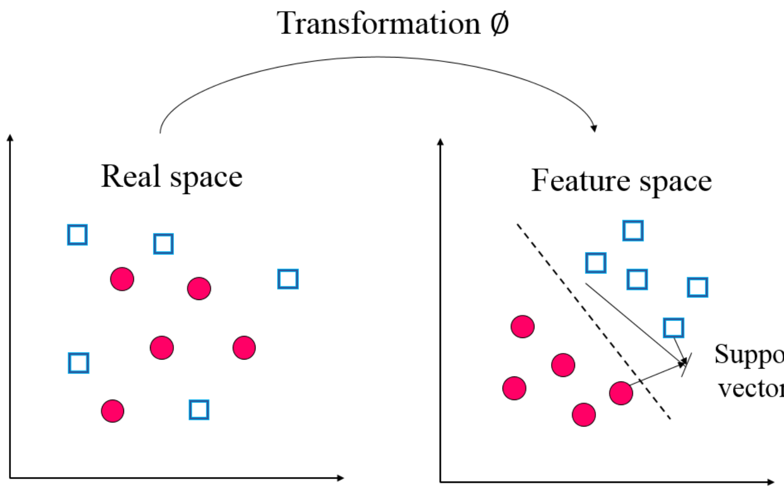

Figure 1: The transformation of the SVM model.

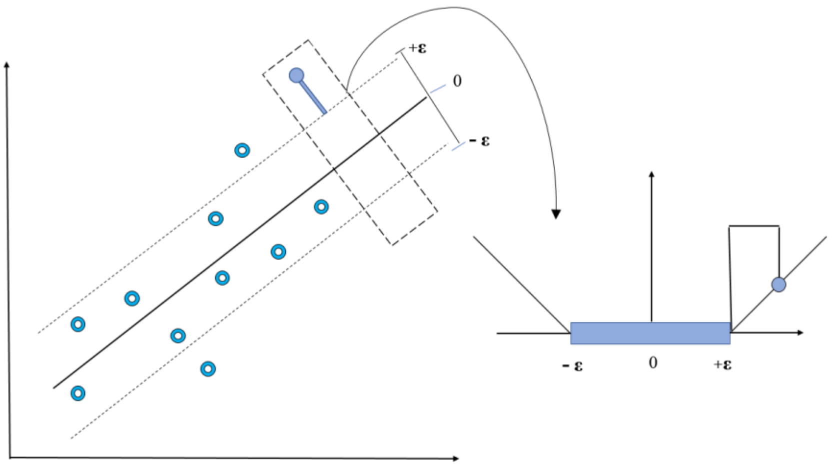

Figure 2. The example of the linear SVM regression model and the ε – insensitive zone

The performance of SVM model is a function of the control parameters (kernel function, C- parameter, and ε – insensitive zone). C-parameter sets the balance between the model complexity and the level of deviation that is larger than ε [52]. The selection of this parameter is by trial and error through the training and testing phases.

Parameter ε is important in fitting the data set during the training phase by setting the width of ε – insensitive. The value of this parameter greatly impacts the support vector regression in SVM model. Kernel function selection is based on the intended application of the model and this can affect the variables during the training phase. The commonly used kernel functions are the Polynomial and Gaussian kernel [53]. In this study, Gaussian kernel is adopted owing to its few parameters compared to polynomial kernel.

$$k(X,X') = \exp(-y.\|X - X'\|^2), y > 0 \tag{1}$$

Different methods was used to select the parameters of SVM model [54]. In this study paper. Parameters C and **ε** are selected by using the grid search algorithm [55].

3.3. Accuracy skills metrics

Machine learning models usually is evaluated using statistical metrics that give an insightful meaning for the predictability potential. Hence, the developed models examined using several statistical metrics including mean absolute percentage error (MAPE), root mean square error (RMSE), mean absolute error (MAE) and Nash-Sutcliffe coefficient. The mathematical explanation can be expressed as follows [56]–[58]:

$$MAPE = \frac{100}{n}\sum_{i=1}^{n}\left|\frac{C_{s(o)} - C_{s(p)}}{C_{s(o)}}\right| \tag{2}$$

$$RMSE = \sqrt{\frac{\sum_{i=1}^{n}(C_{s(o)} - C_{s(p)})^2}{n}} \tag{3}$$

$$MAE = \frac{\sum_{i=1}^{n}\left|C_{s(o)} - C_{s(p)}\right|}{n} \tag{4}$$

$$NSE = 1 - \left[\frac{\sum_{i=1}^{n}(C_{s(o)} - C_{s(p)})^2}{\sum_{i=1}^{n}((C_{s(o)} - \overline{(C_{s(o)}})^2}\right] \tag{5}$$

where *n* represents the number of data sets, $C_{s(o)}$ and $C_{s(p)}$ refer to the actual observations and predicted concrete compressive strength over the training and testing modeling phases.

4. Results and discussion

This section deals with the potential predictability examination of the applied ML models including random forest and support vector machine for predicting concrete compressive strength. Artificial intelligence models were applied in this research to provide an intelligence model that is able to comprehend the actual mechanism of the C_s and the related parameters. ML models were utilized to calculate the mathematical relationship between seven attributes (i.e., $\mathrm{T, w/b, GGBFS/B, W, FA, CA, SP}$) and the predicted variable compressive strength (C_s). Based on several statistical metrics of measurement, the performance of examined ML models were evaluated.

The selection of input variables was utilized in this study to investigate the combination of input variables which control the prediction process. This approach is useful in determination of the variables which have a great impact on the concrete compressive strength, these combinations are shown in Table 1. Seven input combinations were constructed based on the statistical correlation between the input parameters and the target $\mathrm{C_s}$. The input combinations are constructed magnitudes of the correlation toward the value of the $\mathrm{C_s}$which are $\mathrm{T} = 0.23, \frac{\mathrm{w}}{\mathrm{b}} = -0.65, \frac{\mathrm{GGBFS}}{\mathrm{B}} = 0.05, \mathrm{W} = -0.38, \mathrm{FA} = 0.04, \mathrm{CA} = -0.1, \mathrm{SP} = 0.3)$ (Table 1).

Table 1. The input combinations constructed to build the predictive ML models for the computation of the compressive strength

Number of inputs	Input combinations
7 inputs	$M1: C_s = f(T, w/b, GGBFS/B, W, FA, CA, SP)$
6 inputs	$M2: C_s = f(T, GGBFS/B, W, FA, CA, SP)$
5 inputs	$M3: C_s = f(T, GGBFS/B, FA, CA, SP)$
4 inputs	$M4: C_s = f(T, GGBFS/B, FA, CA)$
3 inputs	$M5: C_s = f(GGBFS/B, FA, CA)$
2 inputs	$M6: C_s = f(GGBFS/B, FA)$
1 input	$M7: C_s = f(FA)$

The performance of the RF and SVM models and the attributes combinations are tableted in Table 2-5, respectively. The outcomes were reported based on performance metrics which evaluated for training and testing phase. Table 2 showed the performance indicators of the RF model over training phase. The results indicated that M1 gained an excellent result using the combination of all input variables. The model achieved minimum MAPE ≈ 0.01 MPa, RMSE ≈ 0.023 MPa, MAE ≈ 0.017 MPa and NSE ≈ 0.96. The outputs of RF model over testing phase are reported in Table 3. The results showed that M4 gave a good performance in the prediction process using the combination of T, GGBFS/B, FA and CA as input variable. The model achieved MAPE ≈ 0.02 MPa, RMSE ≈ 0.05 MPa, MAE ≈ 0.03 MPa and NSE ≈ 0.86.

Table 2. The statistical performance measures for the RF model over the training phase.

	MAPE	RMSE	MAE	NSE
RF-M1	0.01118	0.02361	0.01763	0.96795
RF-M2	0.01206	0.02543	0.0191	0.96281
RF-M3	0.01338	0.0292	0.02116	0.951
RF-M4	0.01345	0.03131	0.02141	0.94365
RF-M5	0.01357	0.03166	0.02151	0.94237
RF-M6	0.02272	0.05307	0.03624	0.83813
RF-M7	0.02653	0.06201	0.04245	0.77895

Table 3. The statistical performance measures for the RF model over the testing phase.

	MAPE	RMSE	MAE	NSE
RF-M1	0.0253	0.05869	0.03903	0.82987
RF-M2	0.0275	0.06196	0.04247	0.81043
RF-M3	0.02525	0.05664	0.03886	0.84157
RF-M4	0.02373	0.05256	0.03664	0.86358
RF-M5	0.02914	0.06708	0.04482	0.77776
RF-M6	0.041648	0.101586	0.064102	0.490332
RF-M7	0.04344	0.10767	0.06746	0.42747

The application of the SVM model showed a different predictability performance for the learning process in terms of the investigated combinations of the input parameters. Table 4 and 5 showed the performance measures of SVM model over training and testing phase, respectively. Again, the results reported that M1 achieved the best prediction results of all input variables over the other models. Statistically, the model accomplished MAPE ≈ 0.02 MPa, RMSE ≈ 0.05 MPa, MAE ≈ 0.03 MPa and NSE ≈ 0.83 for training phase. For testing phase, the best model gave MAPE ≈ 0.03 MPa, RMSE ≈ 0.06 MPa, MAE ≈ 0.04 MPa and NSE ≈ 0.82. The best performance is acquired using all inputs variables while RF model achieved a better performance with 4 inputs combination. It can be noticed that RF model has a better performance than SVM model and this is returned to its capability in handling complex system [59]. The comparison of two models showed that RF model showed the superiority of RF model in terms of performance measures metrics.

Table 4. The statistical performance measures for the SVM model over the training phase.

	MAPE	RMSE	MAE	NSE
SVM-M1	0.02402	0.05419	0.03754	0.83118
SVM-M2	0.02593	0.05828	0.0404	0.80472
SVM-M3	0.02911	0.06963	0.04539	0.72132
SVM-M4	0.03365	0.08155	0.05268	0.61769
SVM-M5	0.036094	0.081941	0.056909	0.61403
SVM-M6	0.0535	0.11368	0.08446	0.25707
SVM-M7	0.05499	0.11744	0.08651	0.20715

Table 5. The statistical performance measures for the SVM model over the testing phase.

	MAPE	RMSE	MAE	NSE
SVM-M1	0.03001	0.06008	0.04662	0.82172
SVM-M2	0.03606	0.07143	0.05577	0.74801
SVM-M3	0.03739	0.0768	0.05793	0.7087
SVM-M4	0.04266	0.08666	0.06673	0.62914
SVM-M5	0.049826	0.097632	0.078341	0.529238
SVM-M6	0.06125	0.12305	0.09536	0.25223
SVM-M7	0.06202	0.12755	0.09602	0.19657

Figures 3 and 4 displayed the scatter plot and the coefficient of determination for the testing phase for the RF and SVM models. Scatter plot used to give a better visualization of the prediction models. The graph describes the relationship between the observed and the predicted variables. Figure 3 indicated that RF M1 gave a superior correlation value with R^2 of 0.94 in comparison with the other models. Whereas, the outcome of the SVM is presented in Figure 4. The outputs showed that best model is M1 with R^2 value equal to 0.93. These results demonstrated an improvement in prediction result with 1% of R^2 which achieved by RF model.

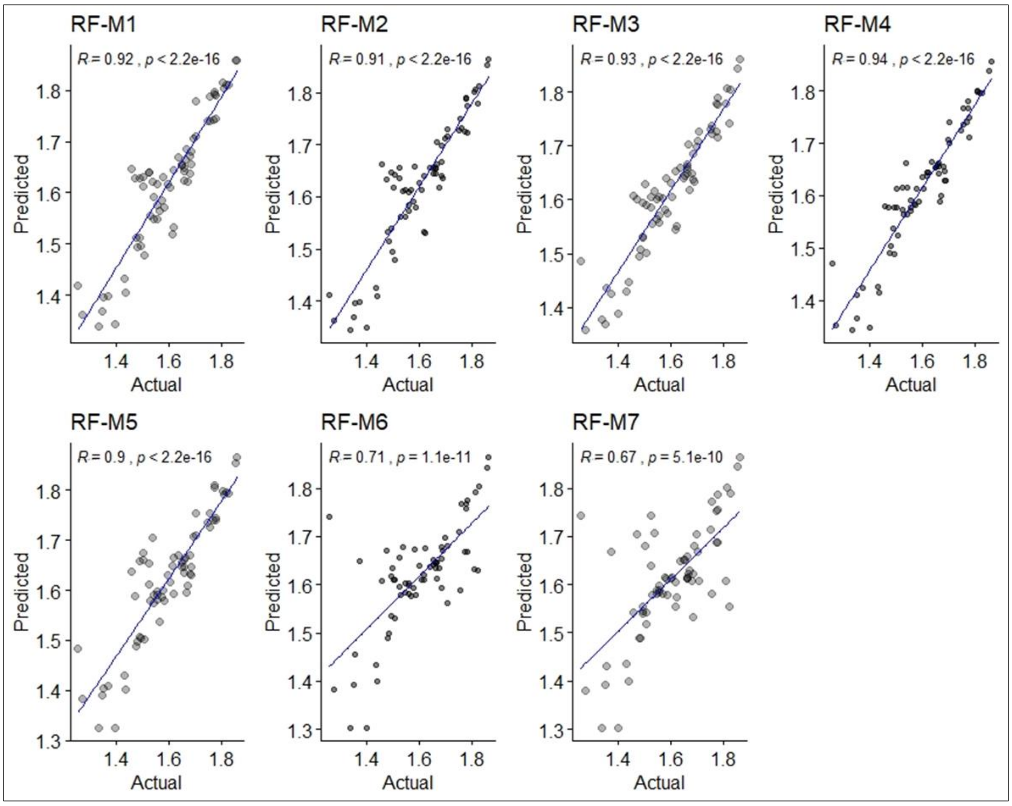

Figure 3. The magnitudes of the correlation of the determination and the scatter plot variation between the actual and predicted C_s over the test modeling phase for RF model and for all investigated input combinations

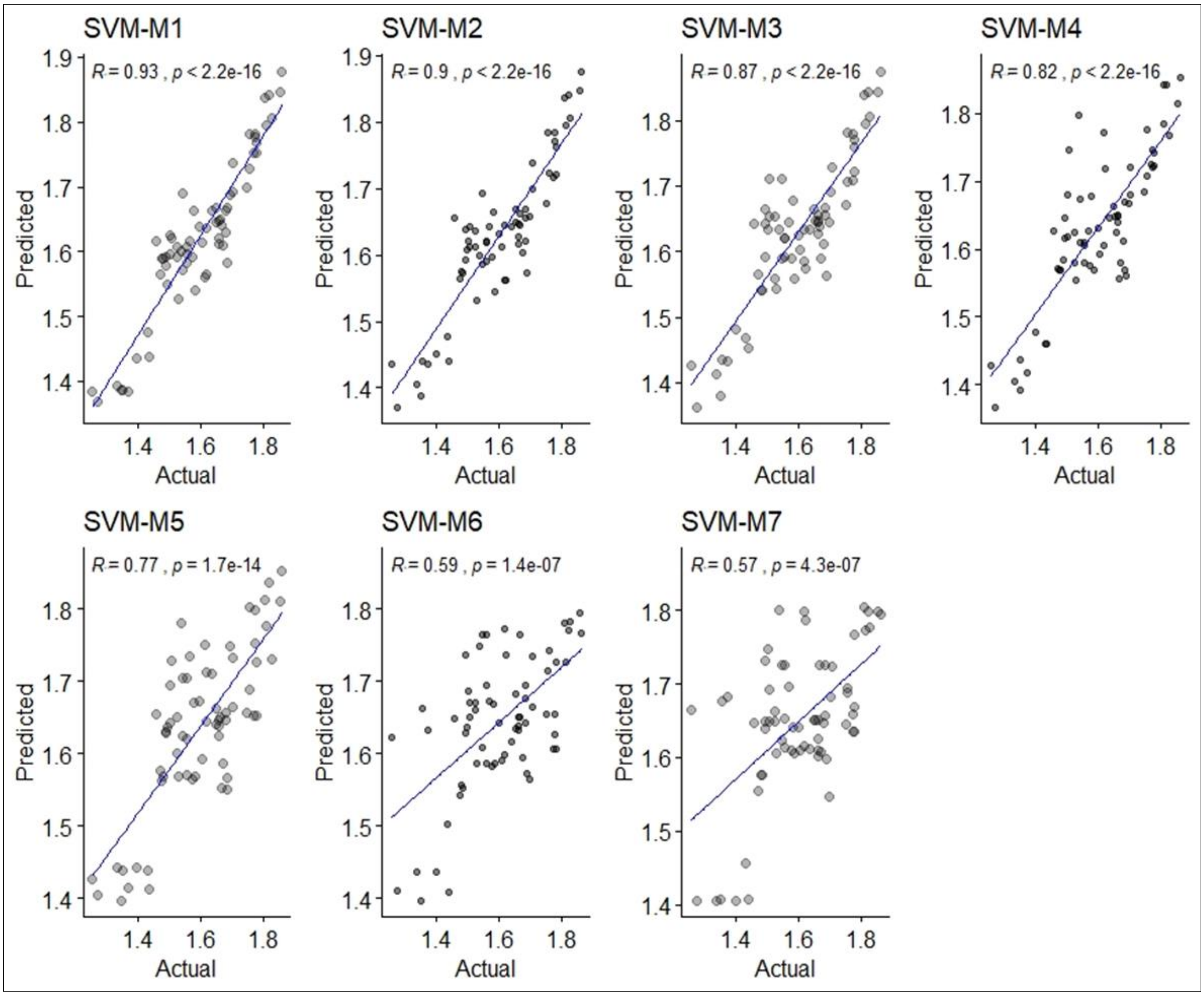

Figure 4. The magnitudes of the correlation of the determination and the scatter plot variation between the actual and predicted C_s over the test modeling phase for SVM model and for all investigated input combinations

Figures 5 and 6 depicted the graphical representation of the three performance indices include root mean square error, correlation and standard deviation in the Taylar diagram. Taylor diagram shows a better presentation of the optimal model combinations that have a nearest distance to the observed compressive strength. Figure 5 was displayed that RF model with M4 variables combination revealed the closest distance to the observed compressive strength. While Figure 6 showed the best variable - combination of SVM model. It could be noticed that SVM model with M1 combination achieved the nearest distance to the observed value. The results indicated that RF model gave a better performance with four input variables than SVM model which gained a good performance with all input variables.

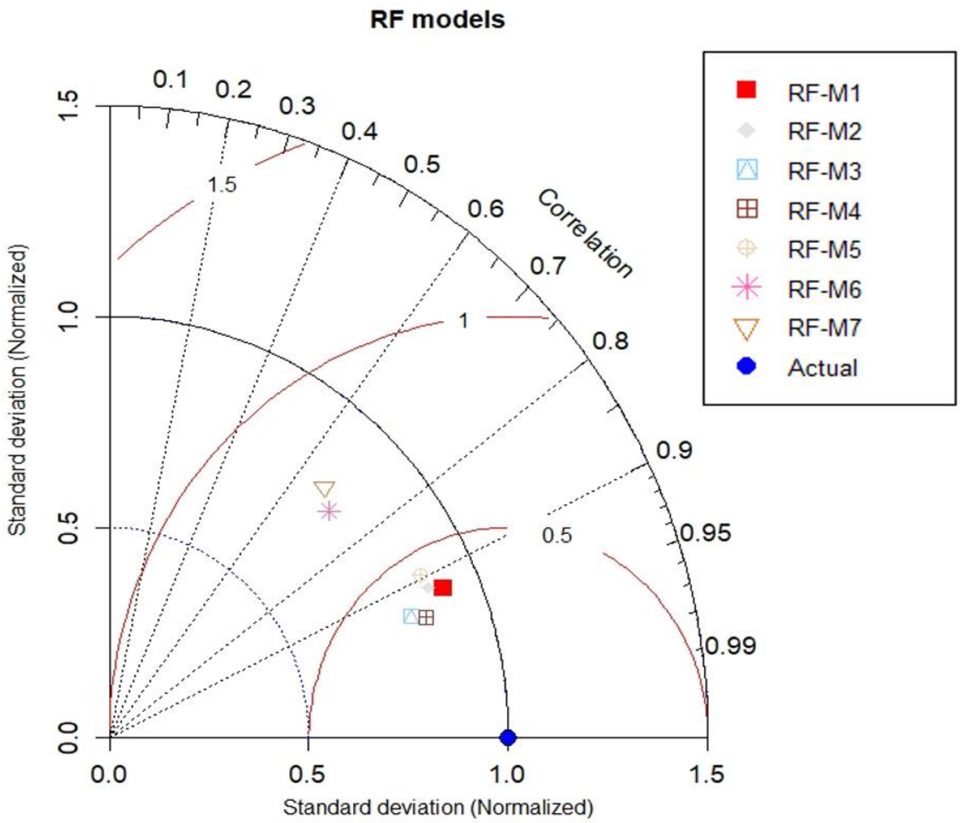

Figure 5. Visualization of the Taylor diagram mapping between the actual and the predicted C_s over the test modeling phase for RF model and for all investigated input combinations.

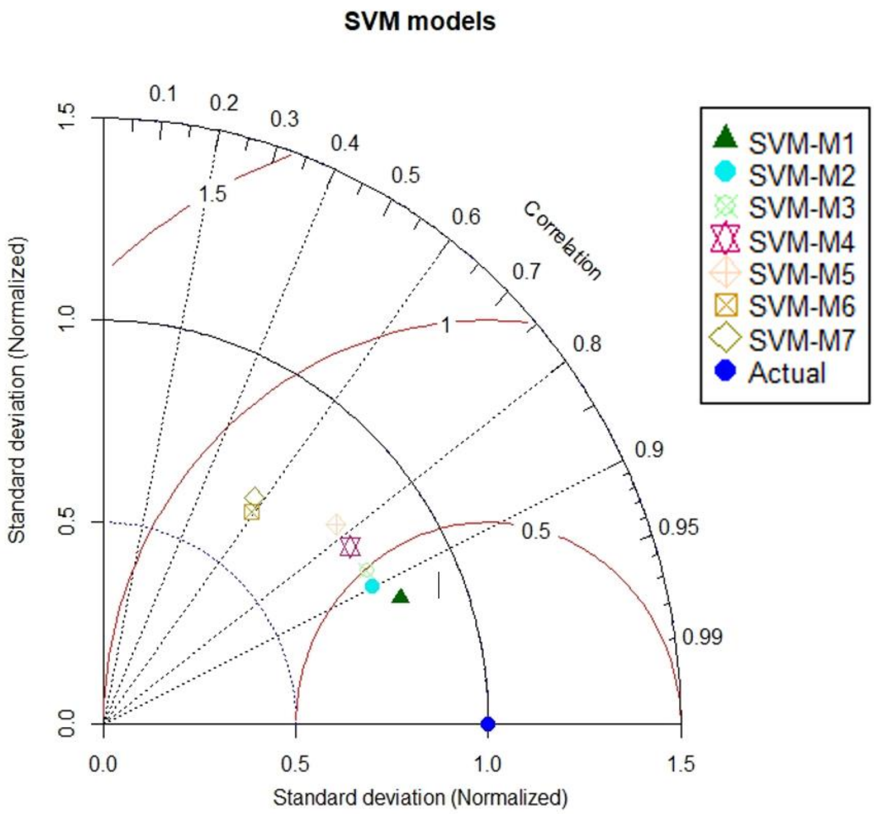

Figure 6: Visualization of the Taylor diagram mapping between the actual and the predicted C_s over the test modeling phase for SVM model and for all investigated input combinations.

Figures 7 and 8 were described the residual error of the ML models and their combination. Figure 7 showed a better visualization of the input combinations performance on testing phase. From this figure, IT can be noticed that RF M4 gave the minimum error for compressive strength prediction with limited error ∓ 3% and less outliers. On the other hand, Figure 8 presented that minimum error gave by SVM M1 with error limited to ∓ 4%.

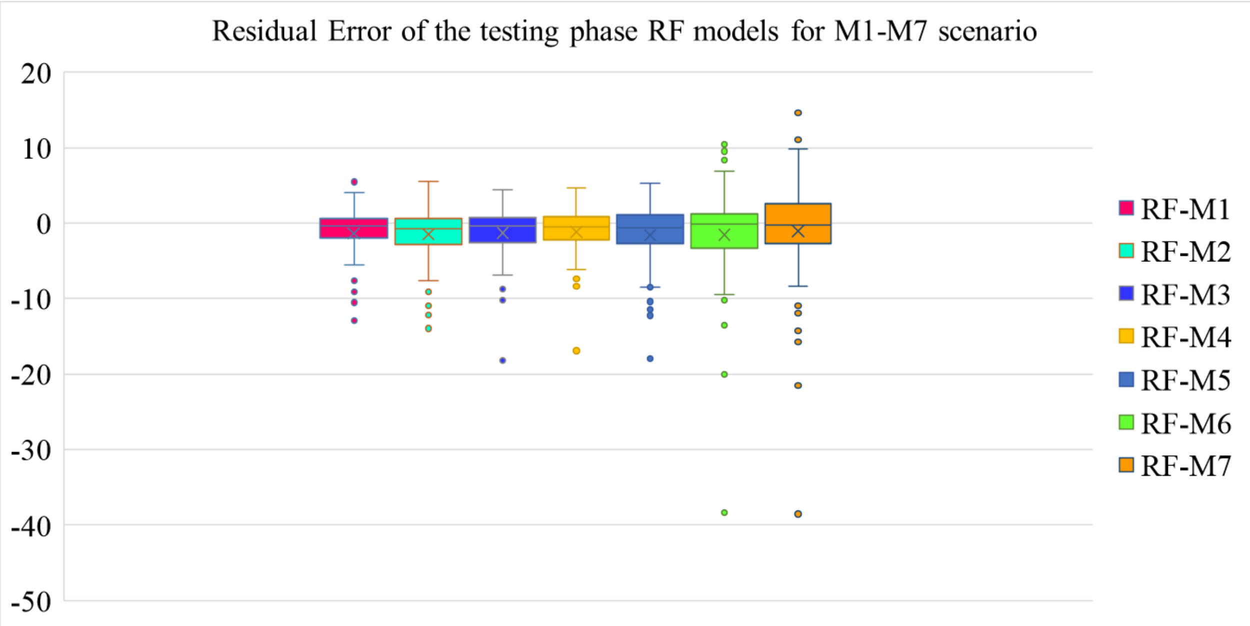

Figure 7. The residual error box plots for the RF predictive model over the testing phase

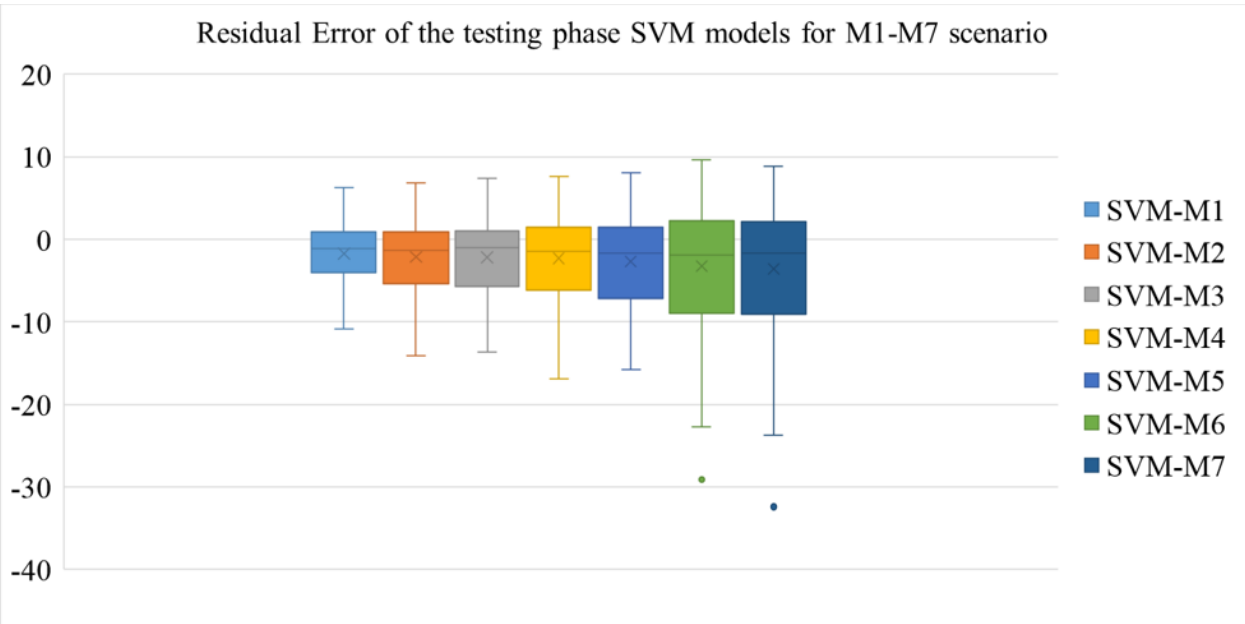

Figure 8. The residual error box plots for the SVM predictive model over the testing phase

The attained predictability performance of the developed ML models (RF and SVM) could be enhanced through the integration of the feature selection for the highly essential input parameters. Among several input selection approaches, the nature inspired optimization algorithms [60]–[62]. Another possibility of prediction augmentation is the proposition of hybrid models where optimization algorithms are coupled for internal parameters tuning [63], [64].

5. Conclusion

The study is conducted on the utilization of recently explored ML model called random forest for modeling compressive strength (C_s) of GGBFSC. The performance of the proposed RF model was validated against support vector machine model. The models were constructed based on collected experimental observations from open source published related researches. The related parameters were T, w/b, GGBFS/B, W, FA, CA and SP. Seven input combination of modeling scenarios were established to build the predictive models. Based on the achieved prediction results, the proposed RF model displayed an excellent performance for predicting the C_s using T, GGBFS/B, FA and CA. Overall, the proposed methodology showed an excellent predictive model that can be utilized for modeling compressive strength of GGBFSC.

Conflict of interest

The scholar of the current research declares no conflict of interest.

Acknowledgements

The author is acknowledged his appreciation to the literature review studies where the data of the current research is developed.

5.1. References

[1] P. J. M. Monteiro, S. A. Miller, and A. Horvath, “Towards sustainable concrete,” *Nature Materials*, vol. 16, no. 7, pp. 698–699, 2017.

[2] A. Kendall, G. A. Keoleian, and M. D. Lepech, “Materials design for sustainability through life cycle modeling of engineered cementitious composites,” *Materials and Structures/Materiaux et Constructions*, 2008.

[3] J. W. Bullard, P. E. Stutzman, L. M. Ordoñez Belloc, E. J. Garboczi, and D. P. Bentz, “Virtual cement and concrete testing laboratory for quality testing and sustainability of concrete,” in *American Concrete Institute, ACI Special Publication*, 2009.

[4] S. C. Pal, A. Mukherjee, and S. R. Pathak, “Investigation of hydraulic activity of ground granulated blast furnace slag in concrete,” *Cement and Concrete Research*, 2003.

[5] Y.-C. Tang, L.-J. Li, W.-X. Feng, F. Liu, and M. Zhu, “Study of seismic behavior of recycled aggregate concrete-filled steel tubular columns,” *Journal of Constructional Steel Research*, vol. 148, pp. 1–15, 2018.

[6] Y. Tang *et al.*, “Real-time detection of surface deformation and strain in recycled aggregate concrete-filled steel tubular columns via four-ocular vision,” *Robotics and Computer-Integrated Manufacturing*, vol. 59, pp. 36–46, 2019.

[7] A. Behnood and E. M. Golafshani, “Predicting the compressive strength of silica fume concrete using hybrid artificial neural network with multi-objective grey wolves,” *Journal of Cleaner Production*, 2018.

[8] S. J. Barnett, M. N. Soutsos, S. G. Millard, and J. H. Bungey, “Strength development of mortars containing ground granulated blast-furnace slag: Effect of curing temperature and determination of apparent activation energies,” *Cement and Concrete Research*, 2006.

[9] D. P. Bentz, “Influence of water-to-cement ratio on hydration kinetics: Simple models based on spatial considerations,” *Cement and Concrete Research*, vol. 36, no. 2, pp. 238–244, 2006.

[10] S. E. Chidiac and D. K. Panesar, “Evolution of mechanical properties of concrete containing ground granulated blast furnace slag and effects on the scaling resistance test at 28 days,” *Cement and Concrete Composites*, vol. 30, no. 2, pp. 63–71, 2008.

[11] A. Cheng, R. Huang, J.-K. Wu, and C.-H. Chen, “Influence of GGBS on durability and corrosion behavior of reinforced concrete,” *Materials Chemistry and Physics*, vol. 93, no. 2–3, pp. 404–411, 2005.

[12] E. Özbay, M. Erdemir, and H. İ. Durmuş, “Utilization and efficiency of ground granulated blast furnace slag on concrete properties – A review,” *Construction and Building Materials*, vol. 105, pp. 423–434, 2016.

[13] H. SONG and V. SARASWATHY, “Studies on the corrosion resistance of reinforced steel in concrete with ground granulated blast-furnace slag—An overview,” *Journal of Hazardous Materials*, vol. 138, no. 2, pp. 226–233, 2006.

[14] A. M. Neville, *Properties of Concrete*. 2011.

[15] A. Oner and S. Akyuz, "An experimental study on optimum usage of GGBS for the compressive strength of concrete," *Cement and Concrete Composites*, vol. 29, no. 6, pp. 505–514, 2007.

[16] V. G. Papadakis and S. Tsimas, "Supplementary cementing materials in concrete," *Cement and Concrete Research*, vol. 32, no. 10, pp. 1525–1532, 2002.

[17] E. Vintzileou and E. Panagiotidou, "An empirical model for predicting the mechanical properties of FRP-confined concrete," *Construction and Building Materials*, vol. 22, no. 5, pp. 841–854, 2008.

[18] M. Azimi-Pour, H. Eskandari-Naddaf, and A. Pakzad, "Linear and non-linear SVM prediction for fresh properties and compressive strength of high volume fly ash self-compacting concrete," *Construction and Building Materials*, 2020.

[19] J. A. Abdalla, R. Hawileh, and A. Al-Tamimi, "Prediction of FRP-concrete ultimate bond strength using Artificial Neural Network," in *2011 4th International Conference on Modeling, Simulation and Applied Optimization, ICMSAO 2011*, 2011.

[20] D. Van Dao, H.-B. Ly, S. H. Trinh, T.-T. Le, and B. T. Pham, "Artificial Intelligence Approaches for Prediction of Compressive Strength of Geopolymer Concrete," *Materials*, vol. 12, no. 6, p. 983, 2019.

[21] K. Yan and C. Shi, "Prediction of elastic modulus of normal and high strength concrete by support vector machine," *Construction and Building Materials*, vol. 24, no. 8, pp. 1479–1485, 2010.

[22] M. H. Mohana, "Reinforced concrete confinement coefficient estimation using soft computing models," *Periodicals of Engineering and Natural Sciences*, vol. 7, no. 4, pp. 1833–1844, 2019.

[23] Z. Dahou, Z. Mehdi Sbartaï, A. Castel, and F. Ghomari, "Artificial neural network model for steel-concrete bond prediction," *Engineering Structures*, vol. 31, no. 8, pp. 1724–1733, 2009.

[24] M. I. Khan, "Predicting properties of High Performance Concrete containing composite cementitious materials using Artificial Neural Networks," *Automation in Construction*, vol. 22, pp. 516–524, 2012.

[25] M. Azimi-Pour and H. Eskandari-Naddaf, "ANN and GEP prediction for simultaneous effect of nano and micro silica on the compressive and flexural strength of cement mortar," *Construction and Building Materials*, vol. 189, pp. 978–992, 2018.

[26] Z. M. Yaseen, H. A. Afan, and M. T. Tran, "Beam-column joint shear prediction using hybridized deep learning neural network with genetic algorithm," in *IOP Conference Series: Earth and Environmental Science*, 2018.

[27] A. A. H. Alwanas, A. A. Al-Musawi, S. Q. Salih, H. Tao, M. Ali, and Z. M. Yaseen, "Load-carrying capacity and mode failure simulation of beam-column joint connection: Application of self-tuning machine learning model," *Engineering Structures*, vol. 194, no. November 2018, pp. 220–229, 2019.

[28] A. A. Al-Musawi, A. A. H. Alwanas, S. Q. Salih, Z. H. Ali, M. T. Tran, and Z. M. Yaseen, "Shear strength of SFRCB without stirrups simulation: implementation of hybrid artificial intelligence model," *Engineering with Computers*, 2018.

[29] L. M. R. Mahmmod, Z. M. R. A. Rasoul, M. S. Radhi, and S. S. Wajde, "Sustainable utilization of polyethylene terephthalate in producing local precast flooring concrete slabs," *Periodicals of Engineering and Natural Sciences*, vol. 7, no. 4, pp. 1990–1995, 2019.

[30] A. Ashrafian, F. Shokri, M. J. T. Amiri, Z. M. Yaseen, and M. Rezaie-Balf, "Compressive strength of Foamed Cellular Lightweight Concrete simulation: New development of hybrid artificial intelligence model," *Construction and Building Materials*, vol. 230, p. 117048, 2020.

[31] C. Bilim, C. D. Atiş, H. Tanyildizi, and O. Karahan, "Predicting the compressive strength of ground granulated blast furnace slag concrete using artificial neural network," *Advances in Engineering Software*, vol. 40, no. 5, pp. 334–340, 2009.

[32] B. Boukhatem, M. Ghrici, S. Kenai, and A. Tagnit-Hamou, "Prediction of Efficiency Factor of Ground-Granulated Blast-Furnace Slag of Concrete Using Artificial Neural Network.," *ACI Materials Journal*, vol. 108, no. 1, 2011.

[33] H. Naderpour and S. A. Alavi, "A proposed model to estimate shear contribution of FRP in strengthened RC beams in terms of Adaptive Neuro-Fuzzy Inference System," *Composite Structures*, 2017.

[34] M. T. Uddin, A. H. Mahmood, M. R. I. Kamal, S. M. Yashin, and Z. U. A. Zihan, "Effects of maximum size of brick aggregate on properties of concrete," *Construction and Building Materials*, vol. 134, pp. 713–726, 2017.

[35] A. Lee, Z. W. Geem, and K.-D. Suh, "Determination of optimal initial weights of an artificial neural network by using the harmony search algorithm: application to breakwater armor stones," *Applied Sciences*, vol. 6, no. 6, p. 164, 2016.

[36] S.-W. Liou, C.-M. Wang, and Y.-F. Huang, “Integrative Discovery of Multifaceted Sequence Patterns by Frame-Relayed Search and Hybrid PSO-ANN.,” *J. UCS*, vol. 15, no. 4, pp. 742–764, 2009.
[37] X. L. Chen, J. P. Fu, J. L. Yao, and J. F. Gan, “Prediction of shear strength for squat RC walls using a hybrid ANN–PSO model,” *Engineering with Computers*, 2018.
[38] H. Moon and H. Shin, “Utilization of ready mixed concrete sludge for improving the strength of concrete with GGBF slag,” *J. Korean Soc. Civ. Eng*, vol. 22, pp. 315–326, 2002.
[39] K.-M. Lee, K.-H. Kwon, H.-K. Lee, S.-H. Lee, and G.-Y. Kim, “Characteristics of Autogenous Shrinkage for Concrete Containing Blast-Furnace Slag,” *Journal of the Korea Concrete Institute*, vol. 16, no. 5, pp. 621–626, 2004.
[40] K. M. Lee, H. K. Lee, S. H. Lee, and G. Y. Kim, “Autogenous shrinkage of concrete containing granulated blast-furnace slag,” *Cement and Concrete Research*, vol. 36, no. 7, pp. 1279–1285, 2006.
[41] Q. Li, Z. Li, and G. Yuan, “Effects of elevated temperatures on properties of concrete containing ground granulated blast furnace slag as cementitious material,” *Construction and Building Materials*, vol. 35, pp. 687–692, 2012.
[42] P. J. Wainwright and N. Rey, “The influence of ground granulated blastfurnace slag (GGBS) additions and time delay on the bleeding of concrete,” *Cement and Concrete Composites*, vol. 22, no. 4, pp. 253–257, 2000.
[43] L. Breiman, “Random forests,” *Machine Learning*, vol. 45, no. 1, pp. 5–32, 2001.
[44] A. Sharafati *et al.*, “The potential of novel data mining models for global solar radiation prediction,” *International Journal of Environmental Science and Technology*, no. 0123456789, 2019.
[45] S. Janitza, G. Tutz, and A.-L. Boulesteix, “Random forest for ordinal responses: prediction and variable selection,” *Computational Statistics & Data Analysis*, vol. 96, pp. 57–73, 2016.
[46] S. P. Kumar and A. Raaza, “Study and analysis of intrusion detection system using random forest and linear regression,” *Periodicals of Engineering and Natural Sciences*, vol. 6, no. 1, pp. 197–200, 2018.
[47] Z. M. Yaseen, M. T. Tran, S. Kim, T. Bakhshpoori, and R. C. Deo, “Shear strength prediction of steel fiber reinforced concrete beam using hybrid intelligence models: A new approach,” *Engineering Structures*, vol. 177, no. April, pp. 244–255, 2018.
[48] P. Cortez, “Data mining with neural networks and support vector machines using the R/rminer tool,” in *Industrial conference on data mining*, 2010, pp. 572–583.
[49] C. Cortes and V. Vapnik, “Support vector machine,” *Machine learning*, vol. 20, no. 3, pp. 273–297, 1995.
[50] A. J. Smola, “Regression estimation with support vector learning machines.” Master’s thesis, Technische Universität München, 1996.
[51] P. Cortez, M. Portelinha, S. Rodrigues, V. Cadavez, and A. Teixeira, “Lamb meat quality assessment by support vector machines,” *Neural Processing Letters*, vol. 24, no. 1, pp. 41–51, 2006.
[52] A. T. C. Goh and S. H. Goh, “Support vector machines: their use in geotechnical engineering as illustrated using seismic liquefaction data,” *Computers and Geotechnics*, vol. 34, no. 5, pp. 410–421, 2007.
[53] L. H. Hamel, *Knowledge discovery with support vector machines*, vol. 3. John Wiley & Sons, 2011.
[54] C.-M. Huang, Y.-J. Lee, D. K. J. Lin, and S.-Y. Huang, “Model selection for support vector machines via uniform design,” *Computational Statistics & Data Analysis*, vol. 52, no. 1, pp. 335–346, 2007.
[55] L. Diop *et al.*, “The influence of climatic inputs on stream-flow pattern forecasting: case study of Upper Senegal River,” *Environmental Earth Sciences*, vol. 77, no. 5, p. 182, 2018.
[56] Z. M. Yaseen *et al.*, “Predicting compressive strength of lightweight foamed concrete using extreme learning machine model,” *Advances in Engineering Software*, 2017.
[57] B. Keshtegar, M. Bagheri, and Z. M. Yaseen, “Shear strength of steel fiber-unconfined reinforced concrete beam simulation: Application of novel intelligent model,” *Composite Structures*, 2019.
[58] S. K. Zamim, N. S. Faraj, I. A. Aidan, F. M. S. Al-Zwainy, M. A. AbdulQader, and I. A. Mohammed, “Prediction of dust storms in construction projects using intelligent artificial neural network technology,” *Periodicals of Engineering and Natural Sciences*, vol. 7, no. 4, pp. 1659–1666, 2019.
[59] Z. S. Khozani *et al.*, “Determination of compound channel apparent shear stress: application of novel data mining models,” *Journal of Hydroinformatics*, 2019.
[60] S. Q. Salih, A. A. Alsewari, B. Al-Khateeb, and M. F. Zolkipli, “Novel Multi-swarm Approach for Balancing Exploration and Exploitation in Particle Swarm Optimization,” in *Recent Trends in Data Science and Soft Computing*, 2019, pp. 196–206.

[61] S. Q. Salih, "A New Training Method based on Black Hole Algorithm for Convolutional Neural Network," *Journal of Southwest Jiaotong University*, vol. 54, no. 3, 2019.

[62] S. Q. Salih and A. A. Alsewari, "A new algorithm for normal and large-scale optimization problems: Nomadic People Optimizer," *Neural Computing and Applications*, pp. 1–28, 2019.

[63] M. A. Ghorbani, R. C. Deo, V. Karimi, Z. M. Yaseen, and O. Terzi, "Implementation of a hybrid MLP-FFA model for water level prediction of Lake Egirdir, Turkey," *Stochastic Environmental Research and Risk Assessment*, pp. 1–15, 2017.

[64] S. Naganna, P. Deka, M. Ghorbani, S. Biazar, N. Al-Ansari, and Z. Yaseen, "Dew Point Temperature Estimation: Application of Artificial Intelligence Model Integrated with Nature-Inspired Optimization Algorithms," *Water*, 2019.